Fly ash as a permeable cap for tailings management: pedogenesis in bauxite residue tailings

Talitha C. Santini[1,2,3,*] and Martin V. Fey[3,4]

[1,*] School of Geography, Planning, and Environmental Management, The University of Queensland, St Lucia, Queensland 4072, Australia, e-mail: t.santini@uq.edu.au
[2] Centre for Mined Land Rehabilitation, The University of Queensland, St Lucia, Queensland 4072, Australia
[3] School of Earth and Environment, University of Western Australia, 35 Stirling Highway, Crawley, WA 6009, Australia
[4] Department of Plant Production and Soil Science, University of Pretoria, Private Bag X20, Hatfield, Pretoria 0002, South Africa

Abstract

Purpose

Closure of tailings facilities typically involves either a 'cap and store' or 'direct revegetation' approach. Both have been used in the management of bauxite residue (alumina refining tailings), with mixed results. This study evaluated the merit of an intermediate approach, using a permeable cap, and examined the pedogenic trajectory of the Technosol.

Materials and methods

Chemical, mineralogical and physical properties of samples from a Brazilian bauxite residue deposit, which had been capped with fly ash 14 years prior and supported a vegetation cover, were compared to evaluate soil formation and pedogenic trajectory of the developing Technosol according to the World Reference Base for Soil Resources. Samples were collected at three points along an elevation gradient, and from 0 to 150 cm below the surface.

Results and discussion

Rainfall leaching was identified as the most important pedogenic process occurring in the tailings, lowering salinity and pH. The Technosol classification was poorly suited to describe the soil materials within the study site because two wastes (fly ash and bauxite residue) were co-disposed in discrete layers.

Conclusions

The permeability of the fly ash cap is key to soil development in these tailings: it provides a suitable medium for plant growth whilst still allowing contact between the tailings and the surrounding environment. The introduction of a novel prefix qualifier,

ordic, would enable more accurate description of layered Technosols. The Technosol at this site is likely to develop towards an Andosol or Ferralsol.

Keywords

Pedogenesis, Red mud, Remediation, Tailings management, Technosols

1. Introduction

Bauxite residue (also known as 'red mud') is an alkaline, saline-sodic tailings material generated during the Bayer process, in which alumina is extracted from bauxite. Between 3 and 4 billion tonnes of bauxite residue are estimated to be currently stored in deposit areas worldwide, with an additional 120 million tonnes generated each year (Power et al. 2011). Once the tailings facility has reached capacity, closure proceeds by either a 'cap and store' or direct revegetation approach. 'Cap and store' approaches to tailings management involve installation of a cap layer consisting of transported soil, compacted clay or other materials, and aim to limit infiltration of rainfall and air in order to minimise generation of potentially problematic leachates, and stabilise the tailings deposit to avoid dust generation or erosion (Mendez and Maier 2008). Potential risks to the surrounding environment are thus contained by preventing ingress of water and air into the tailings. At the other end of the spectrum, direct revegetation involves amending the tailings such that they can support a plant cover being established in the tailings material itself. Both approaches have been used in the management of bauxite residue tailings, with mixed results (Grafe and Klauber 2011). The high pH (10–13), salinity (electrical conductivity ≥4 mS cm^{-1}) and high bulk density (1.6–3.5 g cm^{-3}) of bauxite residue is a major impediment for both management approaches, with capillary rise of alkaline saline pore water from bauxite residue into caps affecting vegetation in capped deposits (Wehr et al. 2006), and slow dissolution of minerals such as sodalite and calcite buffering pH and sodium concentrations at moderate to high values in amended bauxite residue (Grafe and Klauber 2011). No studies to date have examined the use of an intermediate strategy between the extremes of 'cap and store' and 'direct revegetation,' using a thinner capping layer that does not prohibit interaction between vegetation and bauxite residue tailings.

Cap and store management strategies limit the potential for in situ remediation of tailings by natural processes such as leaching, atmospheric carbonation/oxidation and desiccation and therefore also limit the potential for soil formation. Direct revegetation approaches take full advantage of natural weathering processes to enhance formation of soil within tailings; however, the tailings often present an environment too harsh to support vegetation survival. Intermediate strategies between cap and store and direct revegetation involve the use of a thinner capping layer that is selected primarily to support plant growth, but that does not prohibit interaction between vegetation and tailings, and that also allows leaching and gas exchange in the tailings. An intermediate approach was employed for the management of bauxite residue tailings at the Saõ Luís alumina refinery in Brazil, using fly ash from the refinery's coal-fired electricity generation plant.

Although fly ash is not commonly used as a capping material, it has found application in agricultural settings to improve fertility of acidic sandy soils by increasing water retention, providing plant available P (Pathan et al. 2003), acting as a liming agent, and providing exchangeable Ca and Mg and sulphate (Aitken et al. 1984). Limitations to its use include high salinity and boron concentration (Aitken et al. 1984). As a growth medium for plants, it requires leaching to remove salts, boron and readily dissolved sources of acidity and alkalinity, and benefits from amendment with organic matter such as sewage sludge to boost labile organic C and N and increase nutrient retention capacity (Haynes 2009). The pH of fly ash leachate can vary from acidic (pH 3–4) to alkaline (pH 11–12), depending on coal composition and combustion conditions (Spears and Lee 2004; Roy and Berger 2011). Neutralisation of alkaline bauxite residue with acidic fly ash is slow, requiring >150 days to reach equilibrium, and would require large fly ash-bauxite residue ratios to achieve circumneutral pH (Khaitan et al. 2009). In the case of the Saõ Luís alumina refinery, fly ash was selected as a capping material on the basis of its ability to sustain plant growth by supplying adequate levels of Ca, Mg, K, Fe and Mo (Fortes 2000), rather than on the basis of its neutralisation potential. The fly ash-capped Saõ Luís bauxite residue deposit area currently supports a tree and shrub cover, with understorey grasses, and has weathered for 15 years since establishment. This bauxite residue deposit area was investigated to evaluate the effect of landscape position on in situ remediation and soil formation in fly ash-capped bauxite residue and identify a likely pedogenic trajectory using World Reference Base for Soil Resources classification (IUSS 2006) for the soil within the bauxite residue deposit area based on weathering behaviour to date.

2. Materials and methods

2.1. Site history and sample collection

The Alumar (Maranhão Aluminium Consortium) refinery in Saõ Luís, Maranhão, Brazil, commenced production in 1984, using bauxite from the Porto Trombetas mine. The climate at the Saõ Luís residue storage area is tropical monsoon (Am) according to the Köppen-Geiger climate classification system (Peel et al. 2007), and the balance between rainfall and evaporation produces a net surplus of 1325 mm/year of rainfall (INMET 2012). Deposition of bauxite residue occurred within the residue storage area (Fig. 1) over the period of 1984–1991. Attempts to establish vegetation directly on the residue surface following cessation of residue deposition were unsuccessful (Fortes 2000). In 1996, a 50-cm thick cap of fly ash was placed over the residue surface (Fortes 2000), and seedlings were introduced by planting (Moura 2008). Vegetation density and species richness has increased over time through seed dispersal from surrounding areas (Moura 2008). The fly ash cap appears to have been successful in providing a suitable plant growth medium; however, studies to date have focused on vegetation health and largely neglected to investigate residue properties.

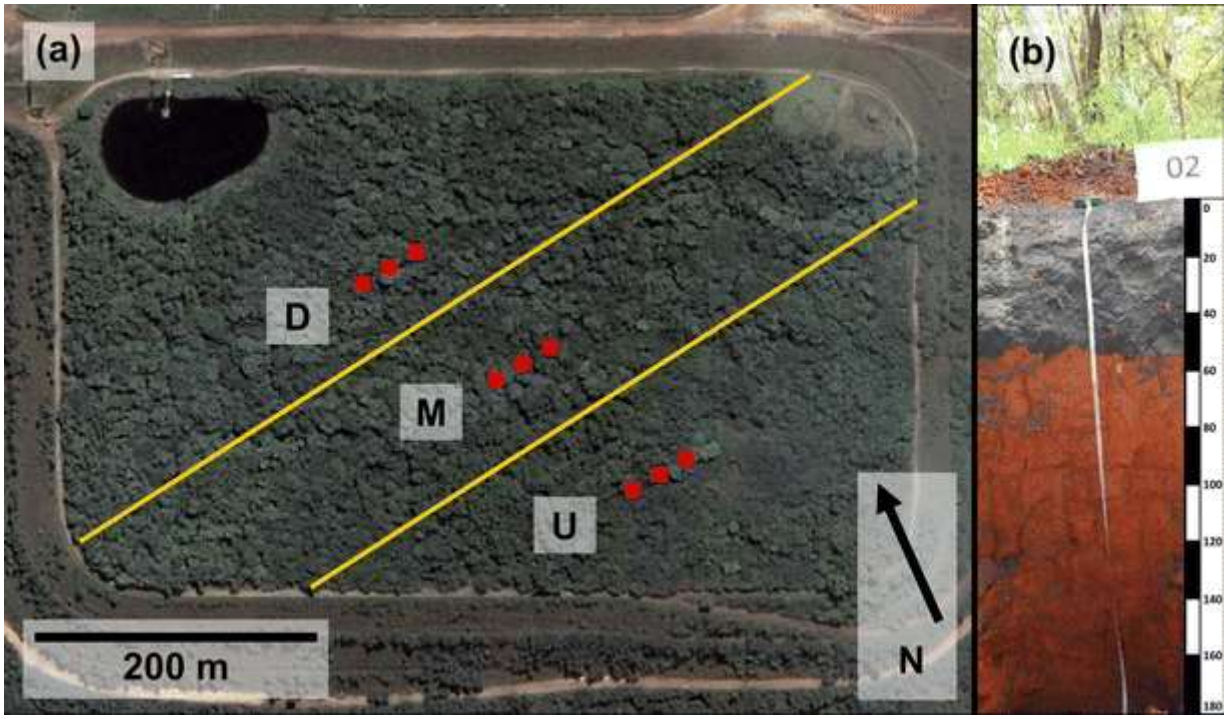

Fig. 1: a Location of pits within fly ash-amended bauxite residue storage area at Saõ Luís. Pits 1, 2 and 3 were located in the upslope (*U*) area; pits 4, 5 and 6 were located in the midslope (*M*) area; and pits 7, 8 and 9 were located in the downslope (*D*) area. The slope between the upslope and downslope pits was approximately 0.5 % (1 m drop in elevation over 200 m in distance).
b Representative soil profile photograph showing black fly ash cap over orange bauxite residue, with desiccation cracks visible throughout the bauxite residue layer

Three elevation areas were identified—upslope, midslope and downslope (Fig. 1)—and in each elevation area, three replicate pits were dug with an excavator to 1 m below the soil surface, and a handheld auger was used to sample below the base of the pit. Samples were collected within the fly ash layer at 0–10 and 40–50 cm below the surface, and then within the residue at 50–60 cm below the surface, and in alternate 10-cm intervals thereafter, to a depth of 2 m below the soil surface. Trees and shrubs dominated vegetation, with some grasses in the understorey, and a 1–2-cm thick litter layer. Vegetation cover was the same at all sites. The fly ash layer appeared to have some topsoil incorporated at pits 4, 5 and 6. Samples were dried at 40 °C to constant weight and then crushed and sieved to <2 mm to remove gravel before chemical and mineralogical analyses.

2.2. Chemical and mineralogical analyses

2.2.1. Chemical analyses

The pH and electrical conductivity (EC) of samples were measured in a 1:5 soil/water extract after 24 h of shaking and 30 min of settling (adapted from method codes 3A1 and 4A1 of Rayment and Higginson 1992 as outlined by Santini et al. 2013a). Total alkalinity content was determined by pH change of a buffer (Dobrowolski et al. 2011). Carbon and nitrogen concentration analyses were only performed on samples from 0 to 10, 40 to 50, 50 to 60, 70 to 80 and 190 to 200 cm depths. Total, organic and inorganic C and N concentrations of samples were

determined by dry combustion (Vario Macro, Elementar Analysensysteme GmbH) before and after acid treatment to remove carbonates (Santini et al. 2013b).

Exchangeable cations and effective cation exchange capacity (ECEC, as sum of cations) were determined by silver thiourea extraction (method codes 15F1 and 15F3, Rayment and Higginson 1992), with a water extraction performed in parallel to correct for soluble salts. Amorphous and poorly crystalline Al, Fe, Si and Ti oxide concentrations were determined by acid ammonium oxalate (AAO) extraction in the dark (method code 13A1, Rayment and Higginson 1992) at a soil/extractant ratio of 1:400 (Santini et al. 2013b). Water, CEC and AAO extracts were all diluted at 1:20 with ultrapure deionised water before analysis by inductively coupled plasma optical emission spectrometry (ICP-OES; Optima 5300DV, PerkinElmer).

2.2.2. Elemental and mineralogical analyses

Total elemental composition of all samples was determined by ICP-OES analysis following fusion and dissolution of samples. A 0.1-g sample was fused with 0.7 g of lithium metaborate-tetraborate (12:22) flux in a Pt crucible at 1050 °C for 45 min, and then the resulting glass bead was dissolved in 7 % HNO_3 by shaking in a capped container for 4 h. Samples were diluted at 1:20 with ultrapure deionised water before ICP-OES analysis.

Samples were prepared for X-ray diffractometry (XRD) by micronizing for 15 min (McCrone Micronising Mill, McCrone Microscopes and Accessories) under ethanol with 5 wt% Si added as an internal standard. After evaporating to dryness, samples were packed into stainless steel plates for the high-throughput stage on beamline 10BM1 of the Australian Synchrotron. X-ray diffraction patterns were collected in transmission geometry, using a wavelength of 0.8240 Å and counting time of 180 s, with rocking of the sample through the omega axis during collection.

2.3. Statistical procedures

Two-way ANOVAs were performed on measured soil properties with site and depth as factors (VSN International 2009). If necessary, data were transformed with a natural logarithm or square root prior to ANOVA to ensure homogeneity of variances. When ANOVA returned significant differences, Tukey's honestly significant difference (HSD) was used as a post hoc test to separate means. A significance level of $\alpha = 0.05$ was used unless otherwise stated. Interactions between depth and site were not significant unless otherwise stated.

3. Results and discussion

3.1. Soil moisture, texture and structure

The downslope site had a lower moisture content than the upslope and midslope sites (Fig. 2), which suggests that drainage rates were limited by proximity to discharge points. According to the USDA soil textural triangle (Soil Survey Division Staff 1993), bauxite residue was classified as coarse sandy loam to coarse sand, and the fly ash was classified as coarse sandy loam to fine sand (data not presented). Fly ash caps contained 3–30 % gravel (cemented, porous, grey

aggregates >2 mm, likely formed by pozzolanic reaction during production) (Fig. 2). A gravel content of ≥40 % is required for classification as *skeletic*; the entire fly ash cap in the downslope site and the 40–50-cm depth of the fly ash cap can be classified as *epihyposkeletic*. There was an average of 10 % gravel in the top 0–10 cm of bauxite residue, and gravel content decreased to <3 % in the remainder of the residue. Gravel may have formed at the top of bauxite residue before application of the fly ash cap as a result of solar drying and cracking. Secondary aluminosilicates and calcite are possible cementation agents (Thompson et al. 1991).

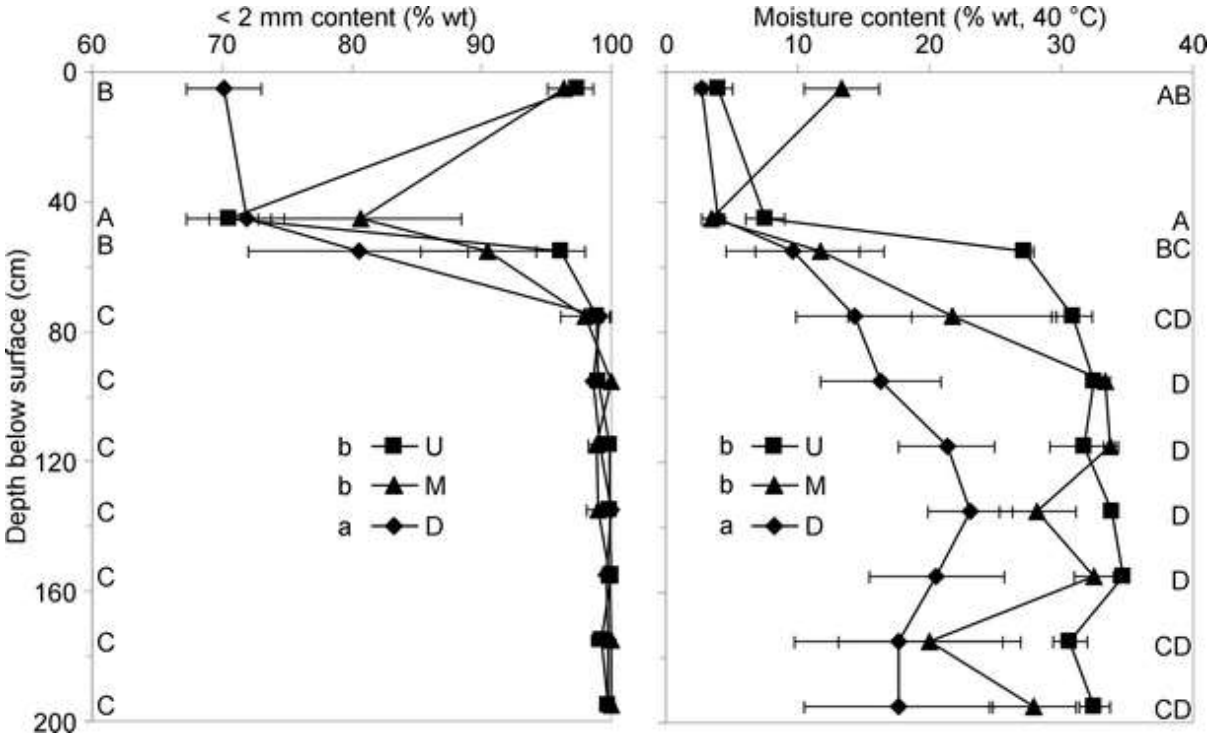

Fig. 2: Concentration of particles <2 mm in diameter ('< 2 mm content') and moisture content in profiles along an elevation gradient within the Saõ Luís bauxite residue storage area. Fly ash caps extended to 50 cm in depth; bauxite residue was present below this depth. Sites are denoted by the abbreviations *U* (upslope), *M* (midslope) and *D* (downslope). Plotted values are the mean of three replicates; *error bars* indicate ± standard error of the mean. *Sites marked with the same lower case letter* in the legend and *depths marked with the same uppercase letter* are not significantly different according to two-way ANOVA (depth × site) at $\alpha = 0.05$. Tukey's HSD was used to separate means

Fly ash layers were generally apedal, although some weak granular root-bound aggregates were observed within the upper 10 cm. The bauxite residue layer had a blocky structure, consisting of firm, angular peds with approximate dimensions ranging from 3 × 3 × 3 to 15 × 15 × 15 cm (Fig. 1b). The structure was strongest within the upslope site and weakened in the midslope and downslope sites. Bauxite residue is typically deposited at 48–55 wt% solids using dry stacking methods (Power et al. 2011); given that bauxite residue was 65–90 wt% solids at the time of collection in this study, volume shrinkage during desiccation is the likely mechanism by which this structure was generated. Rapid initial water loss and volume shrinkage has been observed in other *Technosol*s and is proposed as a unique feature of Technosol weathering associated with *technic* parent materials of initial high water content (Séré et al. 2010).

3.2. Soil chemical analyses

3.2.1. pH, EC and total alkalinity

Significant interactions existed between site and depth for pH; in the upslope and downslope sites, the pH of the fly ash caps between 0 and 50 cm was lower than that of the bauxite residue below the 70–80-cm depth, while in the midslope site, the pH of the fly ash caps between 0 and 50 cm was lower than the residue in the rest of the profile (Fig. 3). The pH of the fly ash caps, where most plant roots were present, was slightly acid to mildly alkaline in terms of the criteria of Hazelton and Murphy (2007). The 50–60-cm depth in the upslope and downslope sites may represent a transition zone between the fly ash cap and the bauxite residue, with fly ash washed into some of the desiccation cracks in residue at this depth. Below 70 cm in the upslope and downslope sites, and below 50 cm in the midslope site, bauxite residue was classified as *alcalic* (IUSS 2006) and very strongly alkaline (Hazelton and Murphy 2007). There were no differences in residue pH between sites or depths below 110–120 cm from the soil surface.

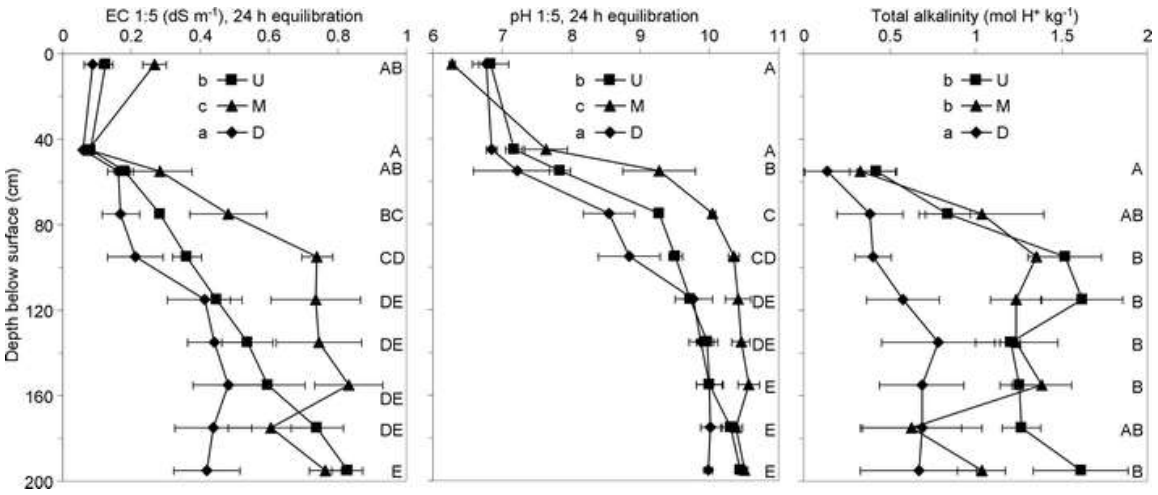

Fig. 3: pH, EC and total alkalinity values in profiles along an elevation gradient within the Saõ Luís bauxite residue storage area. Fly ash caps extended to 50 cm in depth; bauxite residue was present below this depth. Sites are denoted by the abbreviations *U* (upslope), *M* (midslope) and *D* (downslope). Plotted values are the mean of three replicates; *error bars* indicate ± standard error of the mean. *Sites marked with the same lower case letter* in the legend and *depths marked with the same uppercase letter* are not significantly different according to two-way ANOVA (depth × site) at $\alpha = 0.05$. Tukey's HSD was used to separate means

Electrical conductivity decreased with depth below surface; EC of fly ash caps was lower than the bauxite residue, and the upper 50 cm of residue had lower EC than the bottom 10 cm of residue (Fig. 3). Using the EC 1:5 to EC_e (saturation extract EC) conversion proposed by Slavich and Petterson (1993), fly ash caps were classified as non-saline to moderately saline, and bauxite residues are moderately to extremely saline. *Salic* horizons were present below 70 cm from the surface in the midslope sites and below 115 cm from the surface in the downslope and upslope sites. Total alkalinity was lower in the top 10 cm of residue than in the bottom 10 cm.

Trends in pH, total alkalinity and EC with depth are consistent with downward movement of alkaline, saline leachates. The lateral movement of leachates appears

to be more complex. The EC of the downslope site was lower than that of the midslope or upslope sites, and EC was highest in the midslope site. Total alkalinity was higher in upslope and midslope sites than downslope sites. The midslope site had higher pH than the downslope site at 50–60, 70–80 and 90–100 cm depths. These patterns were unexpected based on previous studies of topography and expected leachate movement from upslope to downslope areas (Khaitan et al. 2010; Wehr et al. 2006). Macropore flow along large desiccation cracks described in Section 3.1 and visible in Fig. 1b is likely to influence the hydrological regime within the bauxite residue and create heterogeneous leaching patterns which may contribute to the irregular pH, EC and total alkalinity distributions between sites.

3.2.2. Total, organic and inorganic C and N

There were significant interactions between the effects of site and depth on total C and N; although total C and N concentrations decreased with depth in all sites, the decreases with depth were most pronounced in the midslope site, where concentrations in the upper 0–10 cm of the profile were higher than in the rest of the profile, and least pronounced in the downslope site, where concentrations in the upper 0–60 cm of the profile were higher than in the lower 190–200 cm of the profile (Fig. 4).

Variation in total N was related to organic matter accumulation and decomposition, because organic N accounted for most of total N in these profiles (Fig. 4), and organic N concentrations in fresh bauxite residues are below detection limits (Chen et al. 2010; Courtney and Harrington 2010). Leguminous plants including *Acacia mangium*, *Mimosa acutistipula* and *Leucaena leucocephala* were selected as part of the initial vegetation mix introduced to the residue deposits after installation of the fly ash cap (Moura 2008), and this appears to have been an effective strategy for stimulating nitrogen accumulation in the cap layer. In the fly ash cap, organic C dominated the C pool, indicating that variations in total C were related to organic matter accumulation and residual coal content in the fly ash. In the bauxite residue, inorganic C dominated the C pool, and variations in total C therefore reflected the calcite concentration of the bauxite residue. This was supported by the increases in pH and total alkalinity with depth (Fig. 3). The dominance of organic C relative to inorganic C in the upper 10 cm of bauxite residue may be due to calcite dissolution at the cap-residue interface and migration of residual coal or leaching of organic C from the fly ash cap.

Total C and N were lower in the 40–50-cm depth of the midslope site than other sites (Fig. 4), which is likely due to the incorporation of soil (without coal) in the fly ash cap at the midslope site. Fly ash caps at all sites qualified as *hyperhumic* (organic C concentration ≥5 wt% in upper 50 cm).

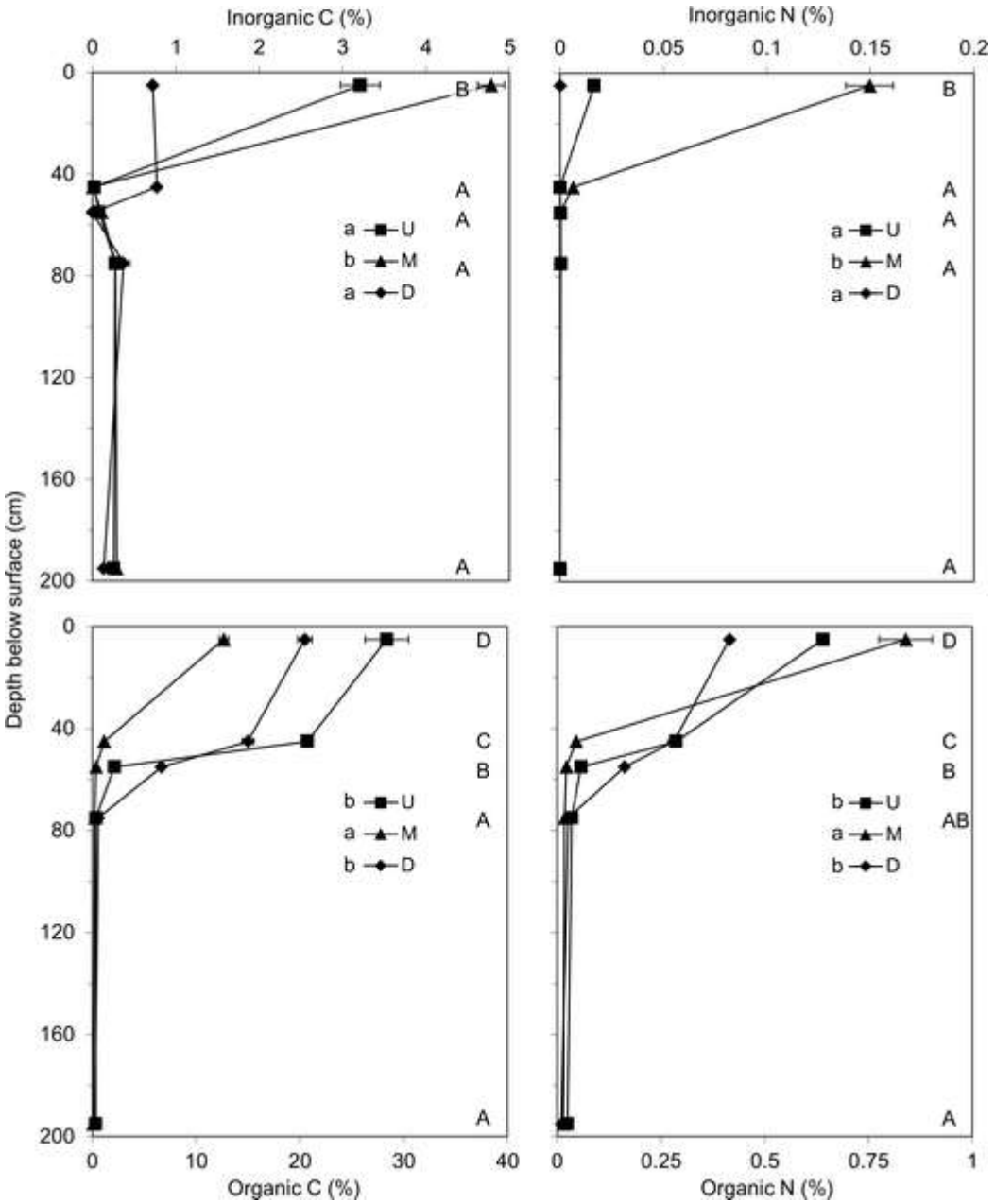

Fig. 4: Inorganic and organic C and inorganic and organic N (% weight) concentrations in profiles along an elevation gradient within the Saõ Luís bauxite residue storage area. Fly ash caps extended to 50 cm in depth; bauxite residue was present below this depth. Sites are denoted by the abbreviations *U* (upslope), *M* (midslope) and *D* (downslope). Plotted values are the mean of three replicates; *error bars* indicate ± standard error of the mean. *Sites marked with the same lower case letter* in the legend and *depths marked with the same uppercase letter* are not significantly different according to two-way ANOVA (depth × site) at $\alpha = 0.05$. Tukey's HSD was used to separate means

3.2.3. Amorphous Al, Fe, Si and Ti oxides

Amorphous oxide concentrations were higher in upslope sites than in downslope sites (Fig. 5); this was unexpected, because leachate export should occur more rapidly in upslope areas and enhance weathering of poorly crystalline minerals. Finer textures were observed in upslope areas; given that amorphous oxides are usually very finely divided, amorphous oxide concentrations may reflect textural variation across the deposit area. Concentrations of amorphous oxides varied little with depth;

amorphous Ti was depleted in the top 0–10 cm of residue, which may be due to eluviation of fine Ti-bearing particulates. Amorphous Al and Si concentration were strongly positively correlated (r = 0.9997***), with an Al:Si ratio of 1.81:1. Allophane (Al:Si commonly between 1:1 and 2:1) and sodalite (Al:Si 1:1) are both removed by the acid ammonium oxalate extractant (Campbell and Schwertmann 1985; Santini et al. 2013b). Patterns in amorphous Al and Si therefore reflect a combination of allophane and sodalite dissolution in the extractant.

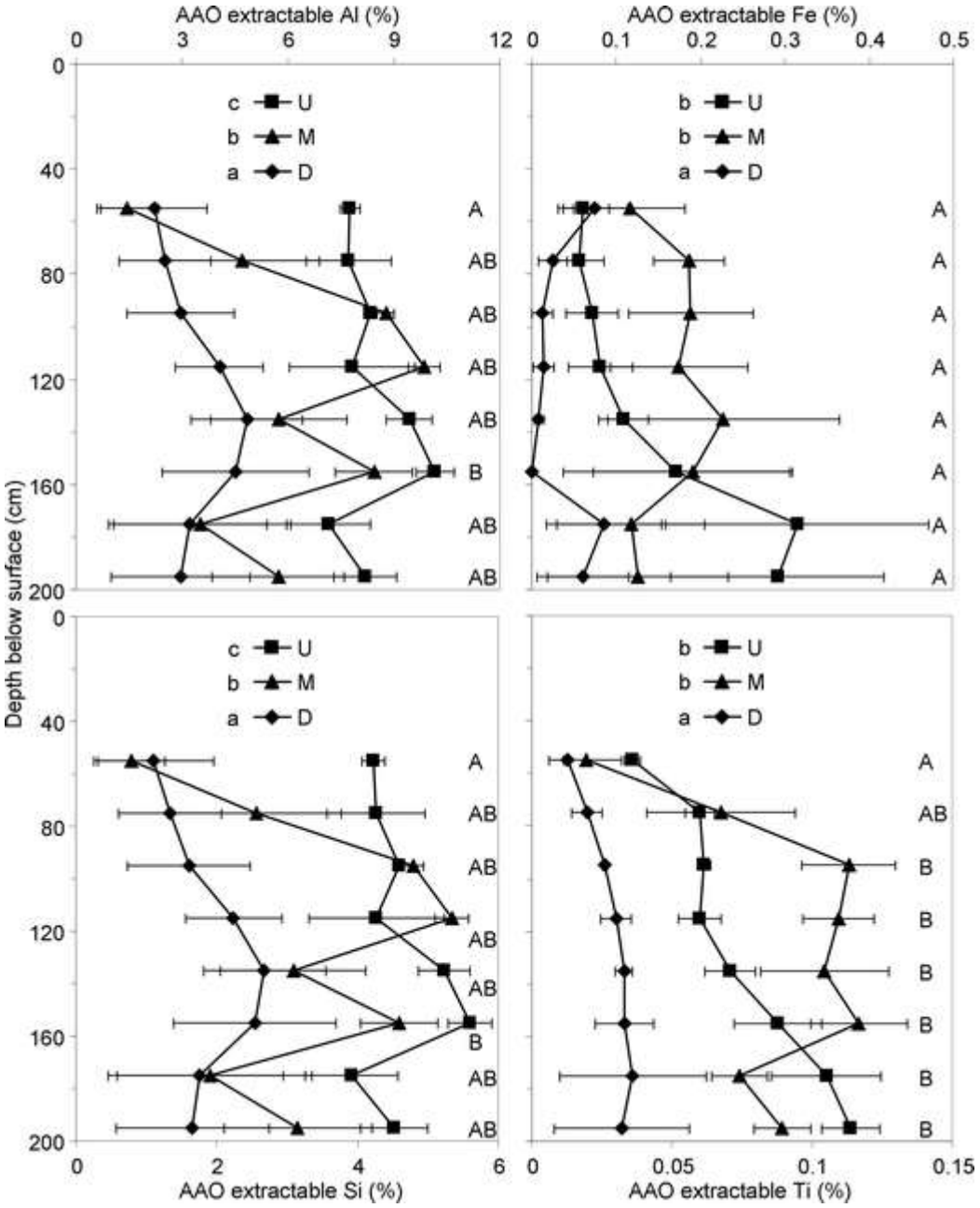

Fig. 5: Amorphous Al, Fe, Si and Ti concentrations (as % element by weight) in profiles along an elevation gradient within the Saõ Luís bauxite residue storage area. Fly ash caps extended to 50 cm in depth; bauxite residue was present below this depth. Sites are denoted by the abbreviations *U* (upslope), *M* (midslope) and *D* (downslope). Plotted values are the mean of three replicates; *error bars* indicate ± standard error of the mean. *Sites marked with the same lower case letter* in the legend and *depths marked with the same uppercase letter* are not significantly different according to two-way ANOVA (depth × site) at $\alpha = 0.05$. Tukey's HSD was used to separate means

3.2.4. Exchangeable cations and effective cation exchange capacity

Effective cation exchange capacity (ECEC) was high in the surface 0–10 cm of profiles, decreased with depth and then increased again at the 190–200-cm depth. This trend in ECEC, as the sum of exchangeable cations, is explained by the dominance of Ca^{2+} in the top 0–10 cm of profiles and Na^{+} at the 190–200-cm depth (Fig. 6). Exchangeable Na^{+} accounted for less than 2 % of ECEC in the upper 50 cm

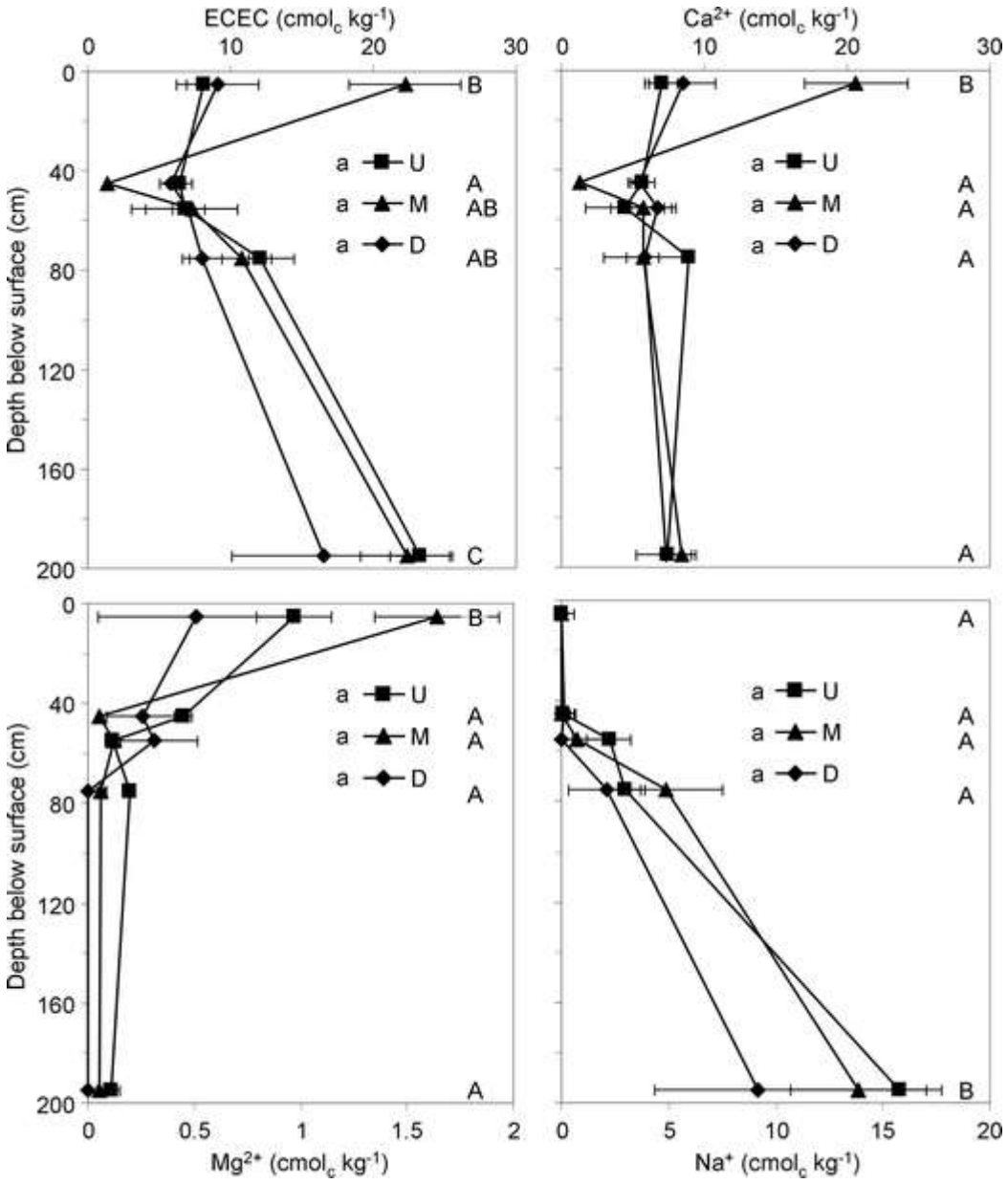

Fig. 6: Effective cation exchange capacity (ECEC) and exchangeable cation (Ca^{2+}, Mg^{2+} and Na^{+}) concentrations in profiles along an elevation gradient within the Saõ Luís bauxite residue storage area. Exchangeable K^{+} was below detection limits and is therefore not shown. Fly ash caps extended to 50 cm in depth; bauxite residue was present below this depth. Sites are denoted by the abbreviations *U* (upslope), *M* (midslope) and *D* (downslope). Plotted values are the mean of three replicates; *error bars* indicate ± standard error of the mean. *Sites marked with the same lower case letter* in the legend and *depths marked with the same uppercase letter* are not significantly different according to two-way ANOVA (depth × site) at $\alpha = 0.05$. Tukey's HSD was used to separate means

and increased with depth in the bauxite residue layers to a maximum of 70 % in the 190–200-cm depth. Exchangeable Ca^{2+} was adequate for plant nutrition, with moderate concentrations available throughout profiles; exchangeable Mg^{2+} was moderate in the surface 0–10 cm and low to very low below this depth (Hazelton and Murphy 2007). No typical symptoms of K or Mg deficiency, such as necrosis in leaf margins and/or tips, interveinal chlorosis or necrotic leaf spots (Mengel et al. 2001), were observed during opportunistic inspection of plant leaves during soil sampling. However, vegetation is likely to benefit from application of a K-rich fertiliser as previously applied in the revegetation study of Moura (2008).

Both EC (see Section 3.2.1) and exchangeable Na^+ increased with depth and have decreased compared to the initial values observed in the bauxite residue (EC 5.7 dS m^{-1}; exchangeable Na^+ 49 $cmol_c\,kg^{-1}$; Moura 2008). This is indicative of leaching, causing soluble salts in the residue to be washed downwards such that *epihyposodic* horizons, with very low exchangeable Na^+, and *endosodic* horizons, with high exchangeable Na^+ and low exchangeable Mg^{2+} can be distinguished, with their junction at 50 cm below the soil surface in the upslope site and 70 cm below the surface in the midslope and downslope sites.

3.3. Elemental and mineralogical composition

3.3.1. Total elemental composition

The major elements present in bauxite residue were Si (25–70 % SiO_2), Fe (15–50 % Fe_2O_3) and Al (10–20 % Al_2O_3); Ti (1.5–4 % TiO_2), Na (0.5–5 % Na_2O) and Ca (0–3 % CaO) were minor elements (Fig. 7). This is a fairly typical composition compared with other bauxite residues, although Si concentrations are higher than average (Grafe et al. 2011; Snars and Gilkes 2009). The parent bauxite had a relatively high kaolinite concentration and low quartz concentration (Bardossy and Aleva 1990), meaning that reactive silica concentration was high, and that the majority of Si in the bauxite residue would be present in sodalite rather than residual quartz. Major elements present in the fly ash caps were Si (50–90 % SiO_2), Al (7–15 % Al_2O_3) and Fe (5–20 % Fe_2O_3), which is consistent with a typical fly ash mineral assemblage dominated by quartz, mullite and hematite (see Section 3.3.2).

Sodium concentration increased with depth in bauxite residue at all sites; rainfall leaching may have flushed Na^+ present in pore water as well as Na^+ from sodalite dissolution downwards (Fig. 6). No Ca enrichment was observed in the bauxite residue profiles, which is consistent with the alkaline pore water environment that would be expected to prevent calcite dissolution. Sodium present in pore water would be transported during leaching, but calcite is unlikely to dissolve to an appreciable extent until pore water pH drops to ca. 8.5. These observations are consistent with a hydrological regime dominated by macropore flow along desiccation cracks as described in Sections 3.1 and 3.2.1. Macropore flow allows rapid leaching along ped faces, but neglects the interior of peds. Initial bauxite residue pore water is high in Na^+ and low in Ca^{2+}, which would be exported rapidly along macropores. Although some calcite present along ped faces would dissolve,

the majority of calcite present in the interior of blocky peds would not be exposed to leaching and little dissolution would be expected to occur.

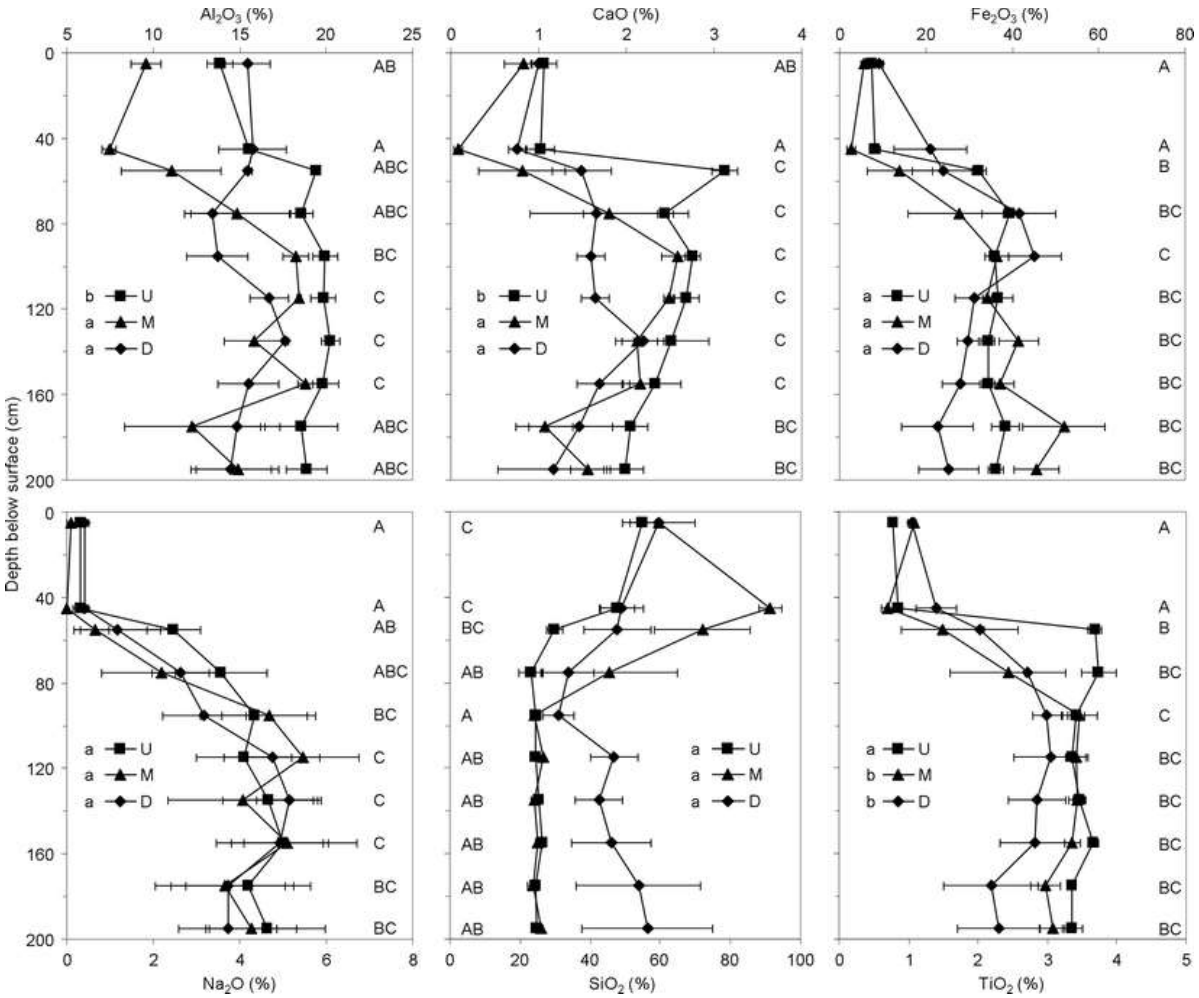

Fig. 7: Total element concentrations (as % weight) in profiles along an elevation gradient within the Saõ Luís bauxite residue storage area. Fly ash caps extended to 50 cm in depth; bauxite residue was present below this depth. Sites are denoted by the abbreviations *U* (upslope), *M* (midslope) and *D* (downslope). Plotted values are the mean of three replicates; *error bars* indicate ± standard error of the mean. *Sites marked with the same lower case letter* in the legend and *depths marked with the same uppercase letter* are not significantly different according to two-way ANOVA (depth × site) at $\alpha = 0.05$. Tukey's HSD was used to separate means

3.3.2. Mineralogical composition

Quartz, hematite, goethite, gibbsite and sodalite were the main minerals present in bauxite residue, and quartz, hematite and mullite were the main minerals present in fly ash (Table 1). These are typical compositions for both materials (Ahmaruzzaman 2010; Grafe et al. 2011; Haynes 2009). The lack of calcium silicate and calcium oxide phases in fly ash is characteristic of a low-calcium fly ash that will not exhibit pozzolanic properties when wet.

Table 1: Minerals present in fly ash cap and bauxite residue samples from the Saõ Luís bauxite residue storage area

Mineral	Chemical formula	Abundance in fly ash cap	Abundance in bauxite residue
Quartz	SiO_2	Major	Major
Hematite	Fe_2O_3	Major	Major
Gibbsite	$Al(OH)_3$	Minor	Major
Goethite	FeOOH	Minor	Major
Mullite	$Al_6Si_2O_{13}$	Major	Minor to trace
Anatase	TiO_2	Trace	Minor
Calcite	$CaCO_3$	Trace to none	Minor to trace
Kaolinite	$Al_2Si_2O_5(OH)_4$	Trace to none	Trace to none
Zircon	$ZrSiO_4$	Trace to none	Trace to none
Rutile	TiO_2	Trace to none	Trace to none
Magnetite/maghemite	Fe_3O_4/Fe_2O_3	Minor	–
Cristobalite	SiO_2	Minor	–
Sodalite	$Na_8(AlSiO_4)_6Cl_2$	–	Major
Boehmite	AlOOH	–	Trace to none

'Major,' 'minor' and 'trace' refers to the averaged composition of all residue samples. Assessment of mineral concentration was made by visual inspection of powder X-ray diffraction patterns

In some profiles, traces of mullite were observed in the upper 10 cm of the bauxite residue (Fig. 8); this indicates that some downward movement of the fly ash may have occurred by illuviation into desiccation cracks in the residue, or by bioturbation which has been observed previously at the site in the form of ant and termite mounds (Moura 2008). However, the presence of gibbsite and minor goethite in the 0–10-cm layer of fly ash in some profiles suggests that some mixing of the residue with the fly ash occurred when the fly ash was initially deposited, which would also account for the presence of traces of mullite in the bauxite residue. Overall, any mixing that may have occurred had a minor effect on the properties of the two layers, because the boundary between layers was visually sharp, and mineralogical analyses revealed only trace contributions of mullite to the bauxite residue XRD patterns, and gibbsite and goethite to the fly ash XRD patterns.

Calcite was present at concentrations of 0.1–0.6 % in residue (based on calculations assuming all inorganic carbon was hosted in $CaCO_3$). Depletion of sodalite and calcite in the upper 50 cm of residue beneath fly ash caps is visible in Fig. 8 by the smaller peak areas of these minerals compared to peak areas from samples deeper below the surface. Sodalite dissolution and leaching would account for part of the observed depletion in Na_2O in these layers (see Section 3.3.1). Although CaO concentration did not change with depth (see Section 3.3.1), calcite concentration appeared to increase with depth (Fig. 8). The Ca^{2+} released during calcite dissolution may have been retained within the soil profile by exchange with Na^+ on soil cation exchange sites (Fig. 6). This would account for the total Ca concentration in the soil remaining constant with depth whilst partitioning of Ca between different pools (solid, exchangeable, dissolved) varies with depth. Depletion of calcium carbonate in the

upper 50 cm of residue, combined with development of soil structure (primarily through desiccation cracking) qualifies this layer as a *cambic* horizon.

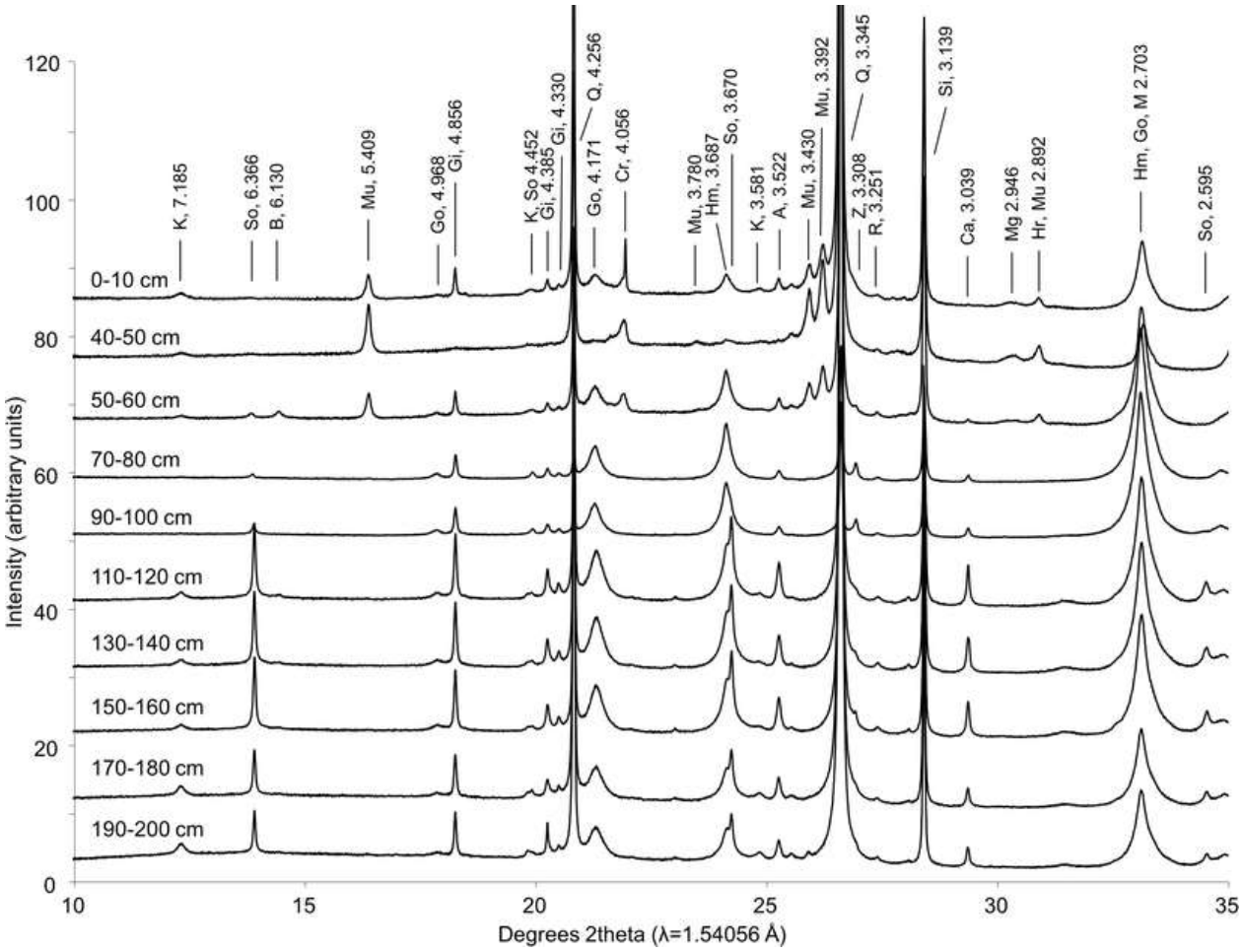

Fig. 8: X-ray diffraction patterns from fly ash and bauxite residue within one representative soil profile within the Saõ Luís storage area. Fly ash caps extended to 50 cm in depth; bauxite residue was present below this depth. Sample depth below surface (0–200 cm) is indicated for each pattern. Peaks between 10 and 35°2θ are labelled with d-spacings (Å) and abbreviations for minerals as follows: *K* kaolinite, *So* sodalite, *B* boehmite, *Mu* mullite, *Go* goethite, *Gi* gibbsite, *Q* quartz, *Cr* cristobalite, *Hm* hematite, *A* anatase, *Z* zircon, *R* rutile, *Si* silicon, *C* calcite and *Mg* magnetite/maghemite

3.4. Soil classification under the World Reference Base and future trajectory

The Saõ Luís site poses problems for classification under the World Reference Base (WRB) due to the multilayered *spolic* profile created by fly ash over bauxite residue. This is a common problem for the classification of Technosols in industrial areas where several tailings or waste types are co-disposed into the same storage facility (Huot et al. 2013, 2014; Séré et al. 2010). The use of a novel prefix qualifier, *ordic*, would improve the clarity of the Technosol classification at sites with multilayered spolic profiles by allowing each spolic layer to be described separately, in parentheses, in order of sequence below the surface. The soils at this site could then

be classified as ordic spolic Technosol (*transportic*, *arenic*, *epihyposkeletic*, *hyperhumic*, *andic*) (*alcalic*, *epicambic*, *sodic*, *endo*/*bathysalic*, *arenic*). Although the specific tests required for WRB classification were not performed on the fly ash samples (AAO extraction, bulk density, phosphorus retention index), the fly ash caps are likely to exhibit andic properties as a result of weathering, as observed in other field-weathered fly ash disposal sites (Zevenbergen et al. 1999; Zikeli et al. 2005).

The bulk residue was classified as arenic; however, *siltic* horizons may develop at depth due to clay illuviation. A blocky structure was visible in the bauxite residue, but little aggregation was observed in the fly ash cap. Further accumulation and decomposition of organic matter from the vegetation cover may aid in structure development within the fly ash cap. The recalcitrant nature of residual organic C in fly ash suggests that organic C will remain high in the fly ash caps, whilst inorganic C is likely to decrease. Parent materials may no longer be recognisable once the fly ash cap develops structure, and pH, EC, total alkalinity and sodalite and calcite concentrations decrease further in the bauxite residue, as have already occurred and have resulted in the development of epihyposalic and epihyposodic horizons in the bauxite residue. Once parent materials are no longer recognisable, the soil could make a transition from the Technosol reference soil group (RSG) to a *Cambisol*.

The Cambisol classification allows for an andic or vitric surface layer and the upper layers of residue already qualify as a cambic horizon because soil structure has begun to develop and calcite has been removed. However, the Cambisol classification does not allow for the presence of buried layers at depths ≥50 cm, or where the newly deposited material can be classified within an RSG other than a *Regosol*. The soil profiles at the Saõ Luís site will therefore likely fit the classification of *Andosol* (epihyposkeletic, hyperhumic, arenic) (*Thapto-Cambisolic*) when they have weathered to the point that the parent materials are no longer readily identifiable.

The increase in ECEC with depth in bauxite residue suggests that further leaching will decrease ECEC throughout the profile and, in combination with clay illuviation, and dissolution of ‘weatherable minerals’ such as sodalite and calcite, cause a ferralic and then a vetic horizon to develop. After transitioning to a Cambisol, if the boundary between the fly ash and bauxite residue remains sharp, the fly ash cap and bauxite residue may develop along separate weathering trajectories, with the fly ash cap developing towards an Andosol and the bauxite residue developing towards a *Ferralsol*. The entire profile could be classified as an Andosol or a Ferralsol in this case, because of the thickness of the fly ash layer (≥30 cm) and the depth of the bauxite residue below the soil surface (≤50 cm). The Andosol classification is the technically correct classification, because of primacy of listing in the WRB Key, the 50-cm thickness of the fly ash cap (which means that the fly ash should be classified as the primary soil material) and the annotation indicating that buried layers are common in the Andosol group, due to the volcanic environments in which they are commonly found. Based on observed changes in response to weathering, and assuming similar behaviour with further exposure, the soil is likely to develop towards an Andosol (arenic) (*Thapto-Ferralsolic*). Andosols are usually highly productive soils, whereas Ferralsols can experience multiple nutrient deficiencies due to their lack of weatherable minerals and low ECEC; both have a tendency for strong P fixation. Monitoring of the soil, and fertilisation where necessary, is

recommended to ensure adequate plant nutrition and establishment of a sustainable vegetation cover.

Classifications involving buried layers fail to capture changes in chemical, mineralogical and physical properties of the bauxite residue in response to weathering; the WRB guidelines should be modified to include provisions for further description of buried layers. Tree roots were observed in the bauxite residue; therefore, the properties of the residue are relevant to surface cover and the behaviour of the soil overall as a medium for plant growth and should be described in the classification of the soil. Allowing the addition of prefix and suffix qualifiers to describe buried layers would be adequate. The fly ash-bauxite residue soil could then be classified as Andosol (hyperhumic, arenic) (Thapto-vetic Ferralsolic (bathysiltic)) in the latter stages of weathering.

4. Conclusions

The behaviour of bauxite residue within the Alumar Saõ Luís storage area demonstrates that a cap and store approach to tailings management that employs a permeable cap can provide a suitable compromise between providing a medium for plant growth and allowing the underlying tailings enough exposure to weathering processes for in situ remediation and soil formation to occur. Rainfall-driven leaching appears to be the main soil-forming process acting upon the bauxite residue tailings, which is expected based on the net surplus of rainfall relative to evaporation at the site. The topography of the site produced different effects than were expected based on previous studies (Khaitan et al. 2010; Wehr et al. 2006); this may be a result of differences in the site water balance and bauxite residue properties between studies.

The multilayered spolic profile created by fly ash over bauxite residue caused problems for classification under the World Reference Base for Soil Resources. Use of the suggested ordic prefix qualifier would improve the clarity of the Technosol classification at this site. The soil at this site would then be currently classified as ordic spolic Technosol (transportic, arenic, epihyposkeletic, hyperhumic, andic) (alcalic, epicambic, sodic, endo/bathysalic, arenic). Assuming weathering behaviour continues along a similar trajectory to that already observed, and with the addition of prefix and suffix qualifiers to describe buried layers, the soil is likely to develop towards an Andosol (hyperhumic, arenic) (Thapto-vetic Ferralsolic (bathysiltic)).

Acknowledgments

Thanks to the team at Alumar Saõ Luís, led by Hezio Oliviera, for sampling and shipping samples for analysis. Thanks also to Stephen Leavy at Alcoa of Australia Ltd for arranging transport of samples and arranging access to and training on analytical equipment. Part of this research was undertaken on the Powder Diffraction beamline (10BM1) at the Australian Synchrotron, Victoria, Australia, and the authors would like to thank Justin Kimpton and Qinfen Gu for assistance with XRD analyses on this beamline. This research was supported by an Australian Postgraduate Award, UWA Geoffrey Kennedy Research Travel Award, and funding from the Minerals and Energy Research Institute of Western Australia, Alcoa of Australia Ltd, and BHP Billiton Worsley Alumina Pty Ltd.

References

Ahmaruzzaman M (2010) A review on the utilization of fly ash. Prog Energy Combust 36:327–363

Aitken RL, Campbell DJ, Bell LC (1984) Properties of Australian fly ashes relevant to their agronomic utilization. Aust J Soil Res 22:443–453

Bardossy G, Aleva GJJ (1990) Lateritic bauxites. Elsevier, Amsterdam

Campbell AS, Schwertmann U (1985) Evaluation of selective dissolution extractants in soil chemistry and mineralogy by differential X-ray diffraction. Clay Miner 20:515–519

Chen CR, Phillips IR, Wei LL, Xu ZH (2010) Behaviour and dynamics of di-ammonium phosphate in bauxite residue processing sand in Western Australia – I. NH_3 volatilisation and residual nitrogen availability. Environ Sci Pollut Res 17:1098–1109

Courtney R, Harrington T (2010) Growth and nutrition of *Holcus lanatus* in bauxite residue amended with combinations of spent mushroom compost and gypsum. Land Degrad Dev 23:144–149

Dobrowolski MP, Fey MV, Santini TC (2011) Rapid determination of residual alkalinity in bauxite residue. Travaux volume 36, 2011 - proceedings of the ICSOBA seminar on bauxite residue (red mud). Mineral Information and Development Centre, Nagpur, pp 38–44

Fortes JLO (2000) Rehabilitation of a bauxite refining residue deposit using industrial waste and leguminous trees. PhD thesis, Universidade Estadual de Maranhão, Saõ Luís, Brazil

Grafe M, Klauber C (2011) Bauxite residue issues: IV. Old obstacles and new pathways for in situ residue bioremediation. Hydrometallurgy 108:46–59

Grafe M, Power G, Klauber C (2011) Bauxite residue issues: III. Alkalinity and associated chemistry. Hydrometallurgy 108:60–79

Haynes RJ (2009) Reclamation and revegetation of fly ash disposal sites—challenges and research needs. J Environ Manag 90:43–53

Hazelton P, Murphy B (2007) Interpreting soil test results: what do all the numbers mean? CSIRO Publishing, Melbourne

Huot H, Simonnot MO, Marion P, Yvon J, De Donato D, Morel JL (2013) Characteristics and potential pedogenetic processes of a Technosol developing on iron industry deposits. J Soils Sediments 13:555–568

Huot H, Simonnot MO, Watteau F, Marion P, Yvon J, De Donato P, Morel JL (2014) Early transformation and transfer processes in a Technosol developing on iron industry deposits. Eur J Soil Sci 65:470–484

Instituto Nacional de Meteorologia (INMET) (2012) Graficos Climatologicos – Saõ Luís. Instituto Nacional de Meterologia, Brasilia

IUSS Working Group WRB (2006) World reference base for soil resources. World soil resources reports no. 103, 2nd edn. Food and Agriculture Organisation of the United Nations, Rome

Khaitan S, Dzombak DA, Lowry GV (2009) Neutralisation of bauxite residue with acidic fly ash. Environ Eng Sci 26:431–440

Khaitan S, Dzombak DA, Swallow P, Schmidt K, Fu J, Lowry GV (2010) Field evaluation of bauxite residue neutralization by carbon dioxide, vegetation, and organic amendments. J Environ Eng 136:1045–1054

Mendez MO, Maier RM (2008) Phytostabilization of mine tailings in arid and semiarid environments-an emerging remediation technology. Environmental Health Perspectives 116:278–283

Mengel K, Kirkby EA, Kosegarten H, Appel T (2001) Principles of plant nutrition, 5th edn. Kluwer Academic, Dordrecht

Moura PA (2008) Phytosociology and natural regeneration of a bauxite residue deposit area revegetated with leguminous trees in Saõ Luís, Brazil. Bachelors Degree (Forestry) dissertation, Universidade Federal Rural do Rio de Janeiro, Rio de Janeiro

Pathan SM, Aylmore LAG, Colmer TD (2003) Properties of several fly ash materials in relation to use as soil amendments. J Environ Qual 32:687–693

Peel MC, Finlayson BL, McMahon TA (2007) Updated world map of the Köppen-Geiger climate classification. Hydrol Earth Syst Sci 11:1633–1644

Power G, Grafe M, Klauber C (2011) Bauxite residue issues: I. Current management, disposal, and storage practices. Hydrometallurgy 108:33–45

Rayment GE, Higginson FR (1992) Australian laboratory handbook of soil and water chemical methods. Inkata, Melbourne

Roy WR, Berger PM (2011) Geochemical controls of coal fly ash leachate pH. Coal Combust Gasification Prod 3:63–66

Santini TC, Fey MV, Smirk MN (2013a) Evaluation of soil analytical methods for the characterisation of alkaline *Technosols*: I. Moisture content, pH, and electrical conductivity. J Soils Sediments 13:1141–1149

Santini TC, Fey MV, Smirk MN (2013b) Evaluation of soil analytical methods for the characterisation of alkaline *Technosols*: II. Amorphous constituents and carbonates. J Soils Sediments 13:1351–1359

Séré G, Schwartz C, Ouvrard S, Renat J-C, Watteau F, Villemin G, Morel J-L (2010) Early pedogenic evolution of constructed Technosols. J Soils Sediments 10:1246–1254

Slavich PG, Petterson GH (1993) Estimating the electrical conductivity of saturated paste extracts from 1:5 soil:water suspensions and texture. Aust J Soil Res 31:73–81

Snars KE, Gilkes RJ (2009) Evaluation of bauxite residues (red muds) of different origins for environmental applications. Appl Clay Sci 46:13–20

Soil Survey Division Staff (1993) Soil survey manual. Agricultural handbook no. 18, soil conservation service, United States Department of Agriculture. United States Government Printing Office, Washington DC

Spears DA, Lee S (2004) The geochemistry of leachates from coal fly ash. In: Giere R, Stille P (eds) Energy, waste, and the environment: a geochemical perspective. Geological Society, London, pp 619–640

Thompson TL, Hossner LR, Wilding LP (1991) Micromorphology of calcium carbonate in bauxite processing waste. Geoderma 48:31–42

VSN International (2009) Genstat release 12.1. VSN International, Helensburgh

Wehr JB, Fulton I, Menzies N (2006) Revegetation strategies for bauxite refinery residue: a case study of Alcan Gove in Northern Territory, Australia. Environ Manag 37:297–306

Zevenbergen C, Bradley JP, van Reeuwijk LP, Shyam AK, Hjelmar O, Comans RNJ (1999) Clay formation and metal fixation during weathering of coal fly ash. Environ Sci Technol 33:3405–3409

Zikeli S, Kastler M, Jahn R (2005) Classification of anthrosols with vitric/andic properties derived from lignite ash. Geoderma 124:253–265